AGN Surveys with FMOS

Masayuki Akiyama[a]

[a]Subaru Telescope, NAOJ, 650 North Aohoku Place, Hilo, HI, 96720, USA

ABSTRACT

The cosmic evolution of the AGN luminosity function provide us unique information on the cosmic growth history of super massive black holes (SMBHs) found in centers of nearby galaxies. Hard X-ray selection of AGNs is one of the most efficient ways to detect various types of AGNs, especially obscured AGNs and low-luminosity AGNs. But, hard X-ray selection is not quite sufficient to detect whole population of AGNs, and multi-wavelength comparison is still quite crucial to understand the whole cosmic growth history of SMBHs accurately. Conducting spectroscopic follow-up observations of multi-wavelength survey fields with high-multiplicity and wide-field of view of FMOS, we can make AGN samples with one to two orders of magnitude larger than hard X-ray AGN sample made so far. Early growth history of SMBHs can be revealed for the first time with high-redshift luminosity function of AGNs made with the sample.

Keywords: AGN, survey, Fibre-MOS

1. INTRODUCTION

With the discovery of super massive black holes (SMBHs) at the center of numbers of massive galaxies,[1] the issue of how these SMBHs formed and evolved over the cosmic history become one of the major question in observational cosmology. The relations between the absolute magnitude of the spheroidal component of galaxy and the mass of their central black hole[2][3][4] or between the stellar velocity dispersion of the spheroidal component and the black hole mass[5][6] imply that close connection between galaxies and their central black holes formation processes. Moreover, the similarity between the cosmic evolutions of star formation rate density and the number density of luminous QSOs suggest that the star formation in galaxy and the black hole growth through accretion of matter peak at the same era in the universe.[7][8]

The luminosity function of AGNs and its cosmic evolution reflects when and where the growth of the SMBH happened via accretion process, i.e., accretion history in the universe. We can convert the luminosity in a certain band to accretion rate with bolometric correction factor (BC) and radiation efficiency ($\epsilon \equiv L_{\rm bol}/(\dot{M}_{\rm acc}c^2)$). The luminous AGNs (QSOs) have similar spectral energy distributions (SEDs) each other,[9] thus assuming a constant BC is not unrealistic. For detailed modeling, bolometric luminosity dependent BC is used.[10] For δ, usually canonical value of 0.1 is assumed. Under these assumptions, the luminosity function of AGNs can be regarded as the accretion rate function. There is a good correlation between black hole mass, which is derived from broad-line width and continuum luminosity, and luminosity for luminous AGNs at various redshifts,[11] this means that the bolometric luminosity ($L_{\rm bol}$) to Eddington luminosity ($L_{\rm E} = 1.5 \times 10^{38}(M_\bullet/M_\odot)$ erg s^{-1}; for ionized gas) ratios (Eddington ratio; $\lambda \equiv L_{\rm bol}/L_{\rm E}$) of luminous AGNs do not distribute in wide range of the value, mostly between 0.1 and 1. The situation may be different for lower luminosity AGNs,[12] but they are not major site of SMBH growth. If we assume the Eddington ratio in addition to the BC, the luminosity of each AGN can reflect the mass of each SMBH. With these assumptions, from the luminosity function, we can estimate the accretion rate and SMBH mass.

Based on the assumptions, the e-folding time scale of black hole growth is $t_{\rm growth} = 3.7 \times 10^7(\epsilon/0.1)(1.0/\lambda)$ yr (Salpeter time), thus, SMBHs can grow 10^4 times in a few handreds Myr time scale, roughly unit redshift interval at $z > 2$ (see Figure 4). Using the continuity equations, we can connect the accretion rate function at different redshifts and estimate the average black hole growth history in the universe.[13] The mass density of the central black holes of galaxies observed in the nearby universe can be explained with the mass accretion happens

Further author information: (Send correspondence to M.A.)
M.A.: E-mail: akiyama@subaru.naoj.org, Telephone: 1-808-934-5962

in AGNs integrated over cosmic time for optically selected AGNs[13] and for hard X-ray selected AGNs.[14] The mass function of SMBHs in the nearby universe is roughly reproduced with assuming that the SMBH merging is negligible and the fraction of galaxies with AGN activity (δ) is 1 at high-redshift ($z = 3$).[10] Based on the consistency, we expect that the major part of the black hole growth happened via accretion, which is detectable as AGNs. Throughout this paper, we use cosmological parameters, $H_0 = 70$ km s^{-1} Mpc^{-1}, $\Omega_M = 0.3$, and $\Omega_\lambda = 0.7$.

2. HARD X-RAY SELECTION OF AGNS

Hard X-ray selection is the most efficient methods to search for various types (radio-quiet/loud, obscured/non-obscured) of AGNs without significant contamination from field galaxies (should be noted that most of the starburst galaxies detected in the deep "hard X-ray" surveys are actually detected only in the 0.5–2 keV soft band). Recent studies on the evolution of the hard X-ray luminosity function of AGNs[15] suggest that the observed black hole mass density in the nearby universe can be roughly explained as a relics of the accretion process observed as the hard X-ray AGNs.[10] This means that the large part of the growth of the SMBHs should be detectable with hard X-ray emission. In the next subsections, we summarize two advantages of the hard X-ray selection, less affected by nuclear obscuration and less contamination from field or host galaxies.

2.1. Obscured Accretion History in the Universe

Spectrum models of the Cosmic X-ray Background (CXB), which is an integrated X-ray emission of various AGNs at wide range of redshifts, imply that about 80% of the accretion process happen in soft-X-ray obscured AGNs/QSOs.[16] Deep optical imaging follow-up observations of the deep hard X-ray survey fields revealed that large fraction of the X-ray sources are *optically-faint* X-ray sources with large hard X-ray to optical flux ratios ($\log f_X/f_R > +1$). The optical counterpart of bright X-ray sources found in the *HEAO1* and *ASCA* surveys are mostly dominated by broad-line AGNs and have $\log f_X/f_R$ typical of them ($0 \sim +1$).[17] On the other hand, in Chandra Deep Field North[18] and Subaru/XMM-Newton Deep Survey field,[19] there are large number of *optically-faint* X-ray sources with $\log f_X/f_R$ more than +1. In the *ASCA* sample the *optically-faint* fraction is only 10%, but it suddenly increases at 1×10^{-14} erg s^{-1} cm^{-2} up to 40% in CDFN and SXDS samples. A new population of optically-faint X-ray sources suddenly emerges at flux level where bulk of the CXB reside. Their contribution to the CXB is significant, i.e., they represent an important part of the growth of the central massive black holes in the galaxies.

Optical spectroscopic observation for part of the *optically-faint* X-ray sources found in the SXDS field is already conducted. For twenty of them we obtained secure identification. A large fraction of them are narrow-emission line AGNs at $z \sim 1$ with strong [OII] and [NV] emission line. There are a few red QSOs and high-redshift narrow line AGN. The X-ray luminosity of these $z > 1$ optically-faint AGNs are more than $L_{2-10\mathrm{keV}} > 10^{44}$ erg s^{-1} cm^{-2}, i.e. large number of obscured QSOs emerged as *optically-faint* X-ray sources in the hard X-ray surveys.

2.2. Low-luminosity AGNs

The hard X-ray selection of AGNs is also efficient to detect low-luminosity AGNs embeded in lumionous host galaxies. In Figure 1, the hard X-ray luminosity function of AGNs is compared with that of optical luminosity function of AGNs derived from 2dF QSO survey (2QZ).[20] The hard X-ray luminosity is converted to optical absolute magnitude with typical optical-to-hard X-ray luminosity ratio (α_{ox}). The luminosity range covered by the hard X-ray AGN sample is shown with the solid lines, and the dashed lines represent the extrapolation of the fitted luminosity function. The hard X-ray data points cover wider luminosity range than those of the optical QSO survey, especially below the knee of the AGN luminosity function.

The wide luminosity coverage of the hard X-ray selection revealed a new aspect of the evolution of the AGN luminosity function. In the right panel of Figure 1, AGN number density in each luminosity bin is shown as a function of redshift. The most luminous sample peaks at $z \sim 2$, same as for the optically-selected AGNs, but, the less luminous sample peaks at lower redshift, at $z \sim 1$. The hard X-ray selected sample is highly complete, thus even if X-ray sources without optical identification is included, still the upper limits on the number density of modest luminosity bin reject that they follow the same evolution as the most luminous AGNs. Similar results

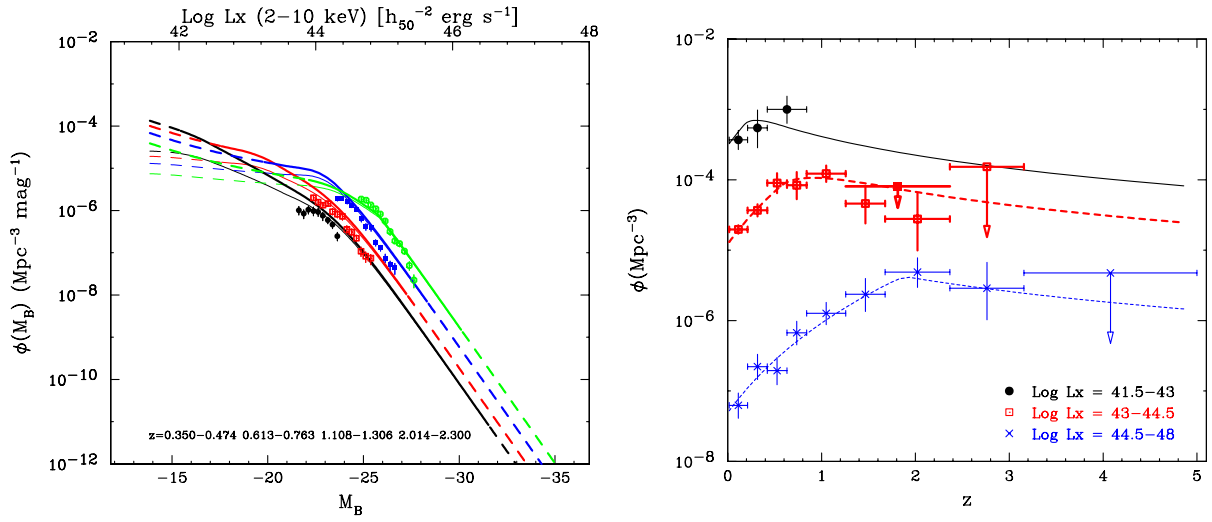

Figure 1. Left) Hard X-ray AGN luminosity function (solid line: fitted luminosity function, covered by sample, dashed line: extrapolation) compared with optical AGN luminosity function from 2QZ (data points; 2dF QSO survey; Boyle et al. 2003) (from Ueda et al. 2003). Right) Number density of hard X-ray selected AGNs in each luminosity bin shown as a function of redshift. The lines indicate the results from luminosity function fitting (from Ueda et al. 2003).

are also reported.[21][22] The difference of the peaks of the luminous and less-luminous AGNs implys that larger black holes stopped their growth at higher redshift on average. Based on the hard X-ray luminosity functions, Marconi et al. (2003) quantitatively evaluates the black hole growth history for low and high mass SMBHs.[10] Considering that the black hole with larger mass reside in the host galaxy with larger spheroidal component, the large SMBHs in large spheroidal system formed earlier than the small SMBHs in small spheroidal system. The results conflict with the hierachical galaxy formation model. But, recent estimate on the star formation history of galaxies as a function of $z = 0$ mass indicates also that the massive galaxies formed at earlier cosmic epoch.[23]

3. IMPORTANCE OF MULTI-WAVELENGTH INFORMATION

3.1. Compton-thick AGNs

The hard X-ray selection is still not quite sufficient to detect the whole population of AGNs. Heavy obscuration with hydrogen column density of $N_{\rm H} > 10^{24}$ cm^{-2}, Compton-thick, can completely hide the central activity of AGNs even in the hard X-ray band. Recent studies on the nearby Seyfert galaxies suggest that there can be a large number of Compton-thick objects, which cannot be seen even in hard X-ray.[24] The number density of Compton-thick AGN population is not clear except for low-luminosity AGNs in the nearby universe. The upper limits derived from the spectrum of the CXB still allow large population of intrinsically luminous Compton-thick AGN population.[15] The fraction of the obscured QSOs at high redshift can be different from that in the nearby universe, because the high-redshift host galaxies of AGNs have more gas and dust. Compton-thick AGNs can be detected using radio, infrared, and sub-mm, selections. For example, mid- and far-infrared observations will detect luminous infrared galaxies at intermediate redshifts, and sub-mm selection is quite efficient to detect the same population at higher redshifts $z \sim 3$. They are galaxies with active nucleus and/or violent star formation, and some of them are Compton-thick AGNs which cannot be detected with hard X-ray selection. It is still crucial to determin the energy source, star burst or AGN for the IR-selected AGN candidates. By comparing AGNs selected in various wavelength, we can estimate the number density of the AGNs which are missed in the hard X-ray selection.

Near-infrared selection of reddened AGN population may also detect another candidates of obscured AGNs which cannot be detected via hard X-ray selection. From 2MASS, 2-Micron All Sky Survey, large number of red

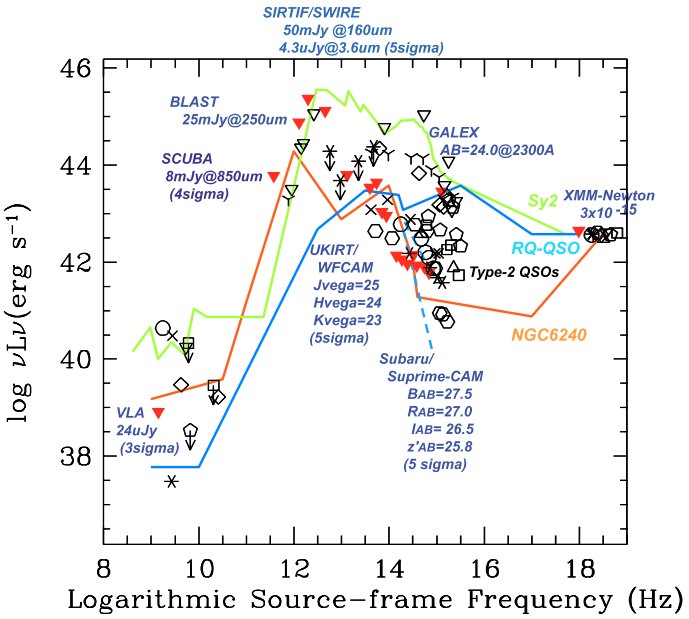

Figure 2. An example of the detection limits of multi wavelength survey (red triangles; Subaru/XMM-Newton Deep Survey) compared with SEDs of radio-quiet QSOs[9] (blue), Seyfert 2 (green), and NGC6240 (orange). Blue dashed line indicates effect of dust absorption to the radio-quiet QSO nucleus with $A_V = 1$ and $A_V = 3$. The SEDs of type-2 QSO candidates are also plotted with black markes. Most of their SEDs are covered by the range of the three solid lines.

QSOs ($J - K_s > 2$) are found at intermediate redshift universe.[25] Follow-up observations with *Chandra* reveal that they are extremely faint in hard X-ray band, X-ray to optical flux ratio is up to 2 orders of magnitudes smaller than usual QSOs.[26]

3.2. Spectral Energy Distribution of AGNs

In addition to use for the AGN selection, the multi-wavelength information is crucial to understand the accretion parameters of SMBHs in each AGN. In order to estimate accretion rate, the bolometric luminosity of each AGN is quite important. The studies on the accretion history so far, mostly use average QSO SED from Elvis et al. (1994)[9] as mentioned above, but the SEDs of QSOs can vary with luminosity and so on. In combination with the SEDs derived from the multi-wavelength dataset, we can accurately determine the SED of each AGN and bolometric luminosity.

An example of the detection limits of multi-wavelength survey, Subaru/XMM-Newton Deep Survey[19] is shown in Figure 2.

4. PROPOSED OBSERVATION

4.1. What We Still Need to Know ?

In order to understand early growth history of the SMBHs, it is important to know the AGN luminosity function (black hole number density and accretion rate distribution) at high-redshift. AGN surveys so far still not sufficient to evaluate the AGN luminosity function, especially its shape, at $z > 3$ universe. Large optical QSO surveys, Sloan Digital Sky Survey (SDSS) and 2QZ (2dF QSO survey), provide only the number density of non-obscured AGNs with high-luminosity end at high-redshift universe.[27] The fraction of obscured AGN is not well known, even at intermediate redshifts, and especially at $z > 1$ universe. The evolution of the fraction of obscured AGN can give us unique crue to connection between QSO formation and galaxy evolution processes.

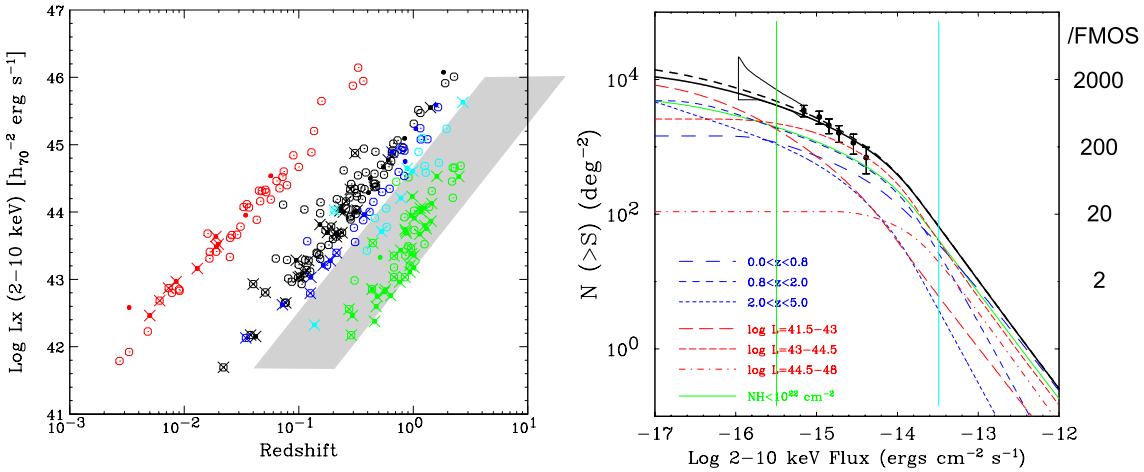

Figure 3. Left) Redshift and luminosity distribution of sample AGNs used in hard X-ray luminosity function derivation in Ueda et al. (2003) (From Ueda et al. (2003) Figure 2). Gray region indicates the redshift vs. luminosity region covered by the FMOS surveys. Right) The cumurative number count in hard X-ray band derived from the extrapolated hard X-ray luminosity function (Original from Ueda et al. (2003) Figure 13b).

4.2. Basic Strategy

The redshift vs. luminosity distribution of AGNs used in the hard X-ray luminosity function study in Ueda et al. (2003)[15] is shown in Figure 3. Important thing to estimate the luminosity function of AGNs efficiently is to cover the redshift vs. luminosity plane throughoutly. If we conduct a large survey with one depth in one field, the obtained sample will distribute along a limited redshift luminosity area can be seen in Figure 3, even in case that the sample size is quite huge. Therefore, the most efficient way is to combine AGN surveys with various depth and area. The minimum number of AGNs to determine the number density in a luminosity bin at a certain redshift with uncertainties of 10% is 100. If we devide the sample into 5 redshift and 5 luminosity bins, we require at least 2500 sample of AGNs to determin the shape and evolution of the luminosity function. The required number can be greatly reduced if we assume continuous redshift evolution and smooth luminosity function, like two power-law model. The number of AGNs used in Ueda et al. (2003) is only 247. On the other hand, in order to evaluate the luminosity function of various types of AGNs (radio-quiet/radio-loud, non-obscured/obscured) independently, the required number will increase.

Another important thing is completeness of the optical identification. At this moment, optical spectroscopic or multi-band photometric information is crucial to determine redshift of each source. In order to examine the redshift distribution of AGNs, 70 $\sim$ 80% completeness is sufficient, but to study the number density of high-redshift AGNs accurately, higher completeness is crucial, because the fraction of high-redshift AGN is not large (for example, about 5% in CDFN for $z > 3$) in the whole sample.

With the low-resolution mode of FMOS, wavelength range from 0.9μm to 1.8μm is covered in one integration. The expected wavelength of strong emission lines observed in AGNs is shown as a function redshift in Figure 4. With the FMOS J-band coverage only, at least one strong emission line is detectable objects at $z > 0.4$. In large fraction of redshift range two emission lines can be detected (shown with yellow areas), and the redshift ranges where only one emission is expected are noted in right side of the Figure.

How far can we reach with FMOS for QSO population ? The SDSS detects several $z \sim 6$ QSOs with absolute magnitude of $M_{1450} > -27.1$ ($M_{\rm B} = M_{1450} + 1.21\alpha + 0.12 = -27.6$ with $\alpha = -0.5$, $f_\nu \propto \nu^\alpha$). The estimated number density of the highest-redshift QSOs is 1/20 of the peak of the QSO number density at $z \sim 2$. Their J-band magnitude are 18 $\sim$ 19, thus with FMOS we can detect 2 to 3 magnitude fainter QSOs, $M_{\rm B} \sim -25$, at the same redshift range. If we extrapolate the observed number dentiy of $M_{1450} > -27.1$ QSOs (1.3×10^{-9} Mpc^{-3}) down to the FMOS detection limit, we expect 10^{-7} Mpc^{-3}, 1 per 1deg^2, i.e. every 5 FMOS FoVs. Large number of such population is only detectable in ultra-wide field survey observation with FMOS.

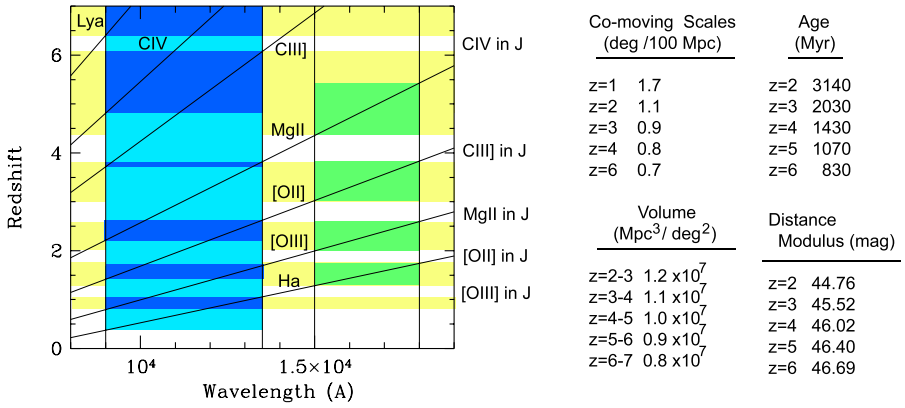

Figure 4. The wavelength of strong emission lines observed in AGNs as a function of redshift. The light blue region indicate the redshift range where at least one emission line is detectable in J-band. For all of the redshift range $z > 0.5$, at least one strong emission line is detectable in the J-band. In dark blue region, two emission line is detectable. The green region, one emission line detectable in H-band. The yellow regions represent the redshift range where at least two strong emission line can be detected.

4.3. Deep Narrow Field (≤ 1 FoV of FMOS)

The deepest hard X-ray survey so far is conducted in the GOODS, Great Origins Observatories Deep Survey, North[28] (CDFN) and South[29] fields. The fields are observed with 2Ms and 1Ms with *Chandra*, respectively. The flux limits reach down to $F_{2-10\mathrm{keV}} = \mathrm{afew} \times 10^{-16}$ erg s^{-1}. Moreover, the fields are covered with multiwavelength surveys from radio to hard X-ray bands. At the hard X-ray flux limit, $\sim$ 80% of the sources have $R < 26$ optical counterpart.[18] The optical spectroscopic identification is only $\sim$60% complete so far. For rest of the X-ray sources without spectroscopic identification, only photometric redshift estimation is available. The estimated photometric redshift distribution indicate large fraction of the X-ray sources without spectroscopic identifications are distribute between $z = 1 \sim 2$. This means that the incompleteness of the spectroscopic identification is partly due to "redshift desert" of the optical spectroscopic observation (see Figure 8 of Barger et al. 2003[18]). Many of them have red optical to near-infrared color, $R - HK'$ colors redder than 5. Thus, near-infrared spectroscopic observation with FMOS is invaluable to reveal the nature of these X-ray sources without spectroscopic identification.

4.4. Deep Wide Field (~ 10 FoVs of FMOS)

For flux limit $F_{2-10\mathrm{keV}} > 10^{-15}$ erg s^{-1} cm^{-2}, the SXDS and Cosmic Evolution Survey (COSMOS) fields will provide us unique samples of X-ray sources selected in wide area. The hard X-ray number count has knee at $F_{2-10\mathrm{keV}} = 1 \times 10^{-14}$ erg s^{-1}, thus the X-ray sources with flux range between $10^{-13} \sim 10^{-15}$ erg s^{-1} cm^{-2} have the largest contribution to the CXB, i.e. the most important population in the black hole growth history.

The X-ray image of the SXDS field is shown in Figure 5. More than 1000 hard X-ray sources are detected in the field. The optical deep imaging observation have been conducted with Subaru/Suprime-Cam down to $B = 27.5$, $R = 27.0$, $i = 26.5$, and $z' = 25.8$ (5σ, AB magnitudes). The survey field is wide, and with

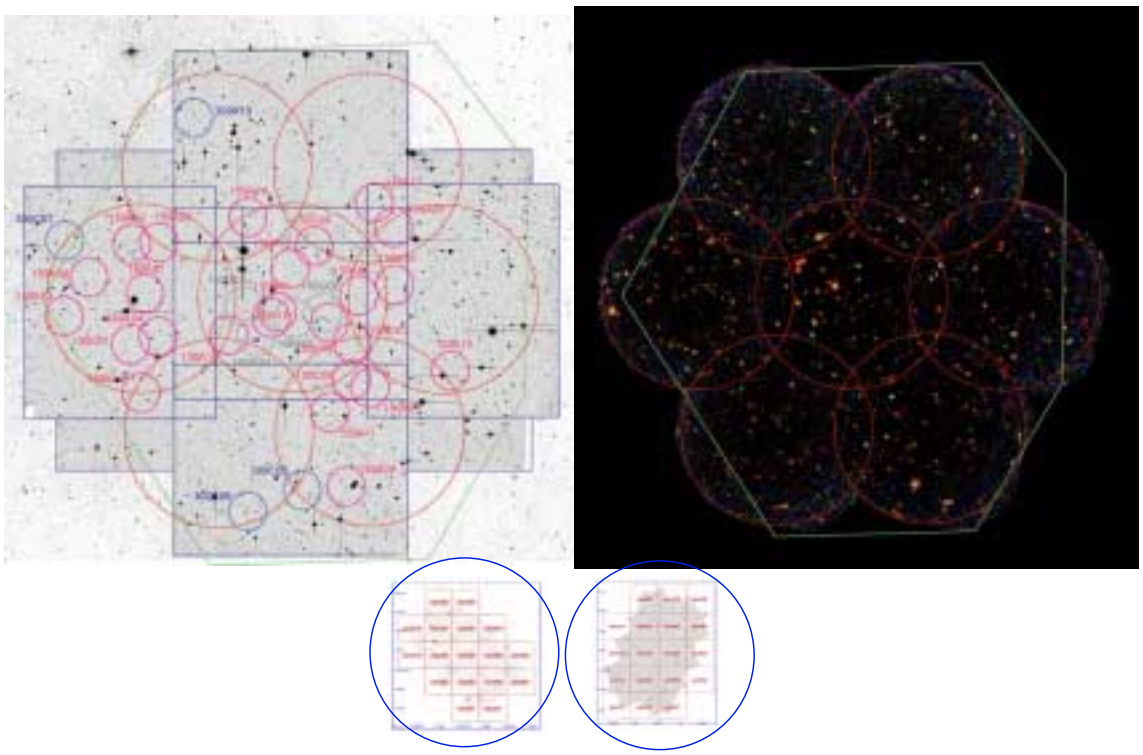

Figure 5. Left) Optical R-band image of the SXDS field taken with Subaru/Suprime-Cam. Right) X-ray image of the SXDS field taken with XMM-Newton. Red (blue) source represent X-ray sources with soft (hard) spectrum. Bottom) Optical image of GOODS North and South in the same scale.

Subaru/FOCAS spectroscopic observations so far only covers 20% of the total area even with 30 FoVs (shown with small circles in Figure 5). Thus, it is crucial to conduct spectroscopic follow-up observation with 8-10m class telescopes with wide FoV MOS instrument. FMOS is the most efficient instrument for this size of area.

4.5. Ultra-wide field (> 100 FoVs of FMOS)

In order to cover the most luminous population of AGNs, it is crucial to cover wide area, because the space density of such AGNs is quite low (10^{-10} Mpc^{-3}). The widest continuous area survey in the hard X-ray band is XMM-Large Scale Survey (XMM-LSS).[30] It is planned to cover $8^\circ \times 8^\circ$ of the sky. In order to cover wide area, serendipitous survey of pointing observation data is also another possibility.[31][32]

Above hard X-ray flux limit of $F_{2-10\mathrm{keV}} > 10^{-14}$ erg s^{-1}, the number density of the source is less than 100 in one field of view of FMOS. Thus, the flux limit is the maximum flux range which can be covered with FMOS efficiently. Above the flux limit, it is better to conduct spectroscopic follow-up observations with wide field of view MOS instrument on 4-m class telescope, like 2dF.

5. TOWARD PHYSICAL UNDERSTANDING OF THE GROWTH HISTORY OF SMBHS

Based on the large number of AGNs at redshift up to 6, we can derive the luminosity function of AGNs and its evolution more accurately. Moreover, we can estimate the black hole mass more directly with broad-line width information obtained from spectroscopic observation than only with luminosity information, that means we do not need to assume a Eddinton ratio to explain the luminosity function of AGNs as mentioned in Section 1. Based on these informations, the black hole accretion parameters, such as ϵ etc., can be constrained.

The large sample of high-redshift obscured QSOs will provide us unique opportunity to directly examine the properties of host galaxies of luminous radio-quiet QSOs at high-redshift and to study the connection between the accretion and the galaxy formation process statistically. For non-obscured QSOs, because the optical nuclear light outshine the host galaxy component, it is impossible to examine the details of host galaxies even with HST (the resolution of the HST PSF corresponds to still 1 kpc scale in the high redshift universe). But, for the obscured QSOs we can directly examine the properties of the host galaxies. With optical to near-infrared follow-up observations of the obscured QSOs, we can estimate star formation rate and stellar mass of the host galaxies. We can also estimate the fraction of galaxies with AGN activity (δ) with comparing the luminosity function of field galaxies and the luminosity distribution of host galaxies at each redshift.[33]

REFERENCES

1. Kormendy,J., & Richstone, D. 1992, ARvAA, 33, 581
2. Magorrian, J., et al. 1998, AJ, 115, 2285
3. Marconi, A., & Hunt, L.K. 2003, ApJ, 589, L21
4. Haring, N, & Rix, H. 2004, ApJ, 604, L89
5. Gebhardt et al. 2000, ApJS, 139, 369
6. Merritt, D., Ferrarese, L. 2001, MNRAS, 320, 30
7. Boyle, B.J., Terlevich, R. J. 1998, MNRAS, 293, 49
8. Franceschini, A., Hasinger, G., Miyaji, T., & Malquori, D. 1999, MNRAS, 310, 5
9. Elvis, M., et al. 1994, ApJs, 95, 1
10. Marconi, A., et al. 2003, MNRAS in press, astro-ph/0311619
11. Corbett, E.A., et al. 2003, MNRAS, 343, 705
12. Sanchez, S.F., et al. 2004, ApJ submitted, astro-ph/0403645
13. Yu, Q., & Tremaine, S. 2002, MNRAS, 335, 965
14. Barger, A.J., et al. AJ, 122, 2177
15. Ueda, Y., Akiyama, M., Ohta, K., & Miyaji, T. 2003, ApJ, 598, 886
16. Gilli, R, Salvati, M., & Hasinger, G. 2001, A&A, 366, 407
17. Akiyama, M., Ueda, Y., Ohta, K., Takahashi, T., Yamada, T. 2003, ApJS, 148, 275
18. Barger, A.J., et al. 2003, AJ, 126, 632
19. Sekiguchi, K., et al. 2003, Multiwavelength Cosmology, in press
20. Boyle, B.J., Shanks, T., Croom, S.M., Smith, R.J., Miller, L., Loaring, N., Haymans, C. 2000, MNRAS, 317, 1014
21. Cowie, L.L., Barger, A.J., Bautz, M.W., Brandt, W.N., & Garmire, G.P. 2004, AJ, 584, L57
22. Hasinger, G., et al. 2004, The restless high energy universe, in press, astro-ph/0310804
23. Heavens, A., Panter, B., Jimenez, R., Dunlop, J. 2004, Nature, 428, 625
24. Risaliti, G., Maiolino, R., & Salvati, M. 1999, ApJ, 522, 157
25. Cutri, R. 2001, AGN Surveys
26. Wilkes, B., et al. 2002, ApJ, 564, 65
27. Fan, X., et al. 2004, AJ, inpress, astro-ph/0405138
28. Alexander, D.M., et al. 2003, AJ, 126, 539
29. Giacconi, R., et al. 2002, ApJS, 139, 369
30. Pierre, M., et al. 2003, A&A, submitted, astro-ph/0305191
31. Watson, M., et al. 2001, A&A, 365, 51
32. Green, P., et al. 2004, ApJS, 150, 43
33. Hamilton, T.S., Casertano, S., & Turnshek, D.A. 2002, ApJ, 576, 61